AUIQ Technical Engineering Science

Manuscript 1062

Toward Faster and Lower-Cost Prosthetic Socket Fabrication: Mechanical Coupon-Level Testing of FDM-Printed PLA/PETG Versus Lamination

Hussein Dhameer Hussein

Wajdi Sadik Aboud

AUIQ TECHNICAL ENGINEERING SCIENCE 2026;3:25–34

ORIGINAL STUDY

Toward Faster and Lower-Cost Prosthetic Socket Fabrication: Mechanical Coupon-Level Testing of FDM-Printed PLA/PETG Versus Lamination

Hussein Dhameer Hussein [a,*], **Wajdi Sadik Aboud** [b]

[a] Department of Prosthetics and Orthotics, College of Engineering, Al-Nahrain University, Baghdad, Iraq
[b] Department of Artificial Intelligence and Robotics Engineering, College of Engineering, Al-Nahrain University, Baghdad, Iraq

ABSTRACT

Additive manufacturing is increasingly being adopted in prosthetic manufacturing because digital workflows can reduce production time and improve repeatability compared to traditional lamination. This study measured two FDM polymers—polylactic acid (PLA) and polyethylene terephthalate glycol (PETG)—against a baseline of Perlon epoxy laminate (not including carbon reinforcement) using standardized coupon tests (n = 3 per test). PLA and PETG samples were printed at 100% fill with a 0.6 mm nozzle, while laminate coupons were prepared by wet layup and cut to the required geometry. Tensile testing followed ASTM D638 and three-point bending followed ASTM D790, modulus, 0.2% offset yield strength, and ultimate strength were derived from stress-strain curves. In tension, PETG showed higher UTS (38.71 ± 1.97 MPa), while PLA showed a slightly higher modulus (0.363 ± 0.104 GPa); The laminate showed lower tensile strength (28.33 ± 2.29 MPa). In bending, PETG achieved the highest bending strength (70.62 ± 3.15 MPa), while PLA showed higher bending stiffness (Ef = 2.07 ± 0.12 GPa) than PETG (1.72 ± 0.02 GPa). To strengthen the technical relevance, a simplified linear elastic finite element model of a three-point bending configuration was demonstrated, confirming the expected midpoint stress concentration and material-dependent deflection. Overall, the findings support evidence-based material screening for prosthetic socket construction, while socket-level validation under standardized structural loading is still needed.

Keywords: Prosthetic socket, FDM, PLA, PETG, Lamination, ASTM testing

1. Introduction

The socket is a vital component of any lower-limb prosthesis with regard to its function, comfort, and acceptance. The prosthetic socket is the main interface to transmit load between the residual limb and the prosthesis and thus, must provide sufficient load distribution, mechanical strength, and long-term stability while maintaining comfort to the user [1, 2]. Poor socket fit or inappropriate material selection can lead to discomfort, skin breakdown, pain, and eventual prosthesis rejection, making socket fabrication one of the most challenging aspects of prosthetic rehabilitation [3]. Conventional fabrication techniques for socket, including the polypropylene process and lamination with resin, perlon, and layers of carbon fiber, have been used for decades and are clinically proven for their strength and reliability [4]. However, these methods are often time-consuming, highly dependent on technician skill, and associated with increased material waste and fabrication cost. In addition, the iterative nature of socket modification in traditional manufacturing can significantly prolong the fitting process, limiting rapid customization for individual patients [5]. Three-dimensional (3D) printing, also known as additive manufacturing, has revolutionized prosthetic development, allowing for the design and fabrication of prosthetic components

Received 16 January 2026; revised 15 March 2026; accepted 10 April 2026.
Available online 4 May 2026

* Corresponding author.
E-mail addresses: hussain.dhameer.pro24@ced.nahrainuniv.edu.iq (H. D. Hussein), wajdisadik@gmail.com (W. S. Aboud).

https://doi.org/10.70645/3078-3437.1062

to be wholly redefined [6]. Unlike conventional fabrication techniques, 3D printing enables the production of complex, patient-specific geometries with high precision and repeatability while significantly reducing fabrication time and material waste [7]. These capabilities have opened new possibilities for rapid prototyping, iterative design, and decentralized manufacturing of prosthetic components [8]. As a result, 3D printing has gained increasing attention for applications in lower-limb prosthetics, where accurate geometry, structural integrity, and efficient production are critical to functional performance and user satisfaction [9]. Alongside these technological advances, a wide variety of materials has been explored for prosthetic fabrication, ranging from traditional laminated composites to thermoplastic polymers used in 3D printing [10]. This material diversity has led to numerous comparative studies aimed at evaluating mechanical performance, durability, and cost. Such investigations remain ongoing, as researchers continue to seek materials that can provide reliable mechanical behavior while reducing manufacturing complexity and overall cost in prosthetic component production [11]. A lot of researchers have already worked with polylactic acid (PLA) to fabricate the prosthesis components, studying their mechanical responses to different manufacturing and test conditions. These studies typically investigated the effect of printing parameters and structural design on mechanical properties, and durability [12–14]. In parallel, polyethylene terephthalate glycol (PETG) has been explored as an alternative thermoplastic material due to its improved toughness and flexibility. Previous studies on PETG-based prosthetic components primarily examined mechanical properties, as well as the effect of printing parameters and material modifications [15–17]. Research has also focused on comparing different materials with respect to their mechanical performance. Investigations of this manner reinforce that material choice is still an area of research within prosthetic socket fabrication [18–20]. Previous studies on prosthetic socket production have often focused either on socket-level strength for specific designs or on material testing limited to a single polymer and a single loading mode. This work contributes a consolidated experimental benchmark by reporting tensile and flexural responses for a Perlon epoxy laminate baseline as well as two widely used FDM polymers (PLA and PETG) within one data set and under a consistent reporting format. By presenting harmonized strain-based calculations (reported as mean ± SD) across three production routes, the study provides a transparent screening reference that can support initial material decisions before socket-level validation is performed. The aim of this study is to preform a coupon-level mechanical screening of 3D-printed PLA and PETG, with that of the conventional laminated composite technique (perlon-epoxy composite). Standardized laboratory test specimens were prepared for each material following ASTM D638 for tensile and ASTM D790 for bending tests. The study seeks to determine which material provides the best balance of strength, durability, and suitability for prosthetic socket applications.

2. Materials and method

In this study, three different material systems were first selected and then evaluated experimentally to ascertain a material system that is most appropriate for prosthetic socket manufacturing. This list contained three materials including two thermoplastics manufactured using additive manufacturing and one composite manufactured traditionally:

- Polylactic Acid (PLA)
- Polyethylene Terephthalate Glycol (PETG)
- Laminated composite material manufactured using the lamination method (twelve layers of Perlon with epoxy)

The mechanical testing was performed under displacement control using standardized coupon specimens. For all tests, the machine output recorded continuous load (kN), cross-head displacement/deformation (mm) and time (s), and these data were used to generate engineering stress-strain (tension) and bending stress-strain (bending). Tensile testing was performed in accordance with ASTM D638 (Fig. 1a), with a machine feed rate setting of 10.0 mm/min. The yield strength was consistently defined using the 0.2% offset method [21]. Three-point bending tests were performed according to ASTM D790 (Method B) (Fig. 1b) with a support span recorded in the machine configuration and a displacement rate setting of 5.0 mm/min. Bending stresses and strains were calculated from recorded load-deflection data using standard ASTM D790 relationships [22]. All results are reported as mean ± SD (n = 3) in SI-consistent units (stress in MPa, modulus in GPa). Because this work is limited to coupon-level tensile and flexural tests under specified ASTM conditions, the findings are for comparative material screening and should not be interpreted as socket-level structural validation without additional component-level validation.

For each material, three tensile specimens were printed. In addition, three bending (flexural) specimens were printed for each material. The printed

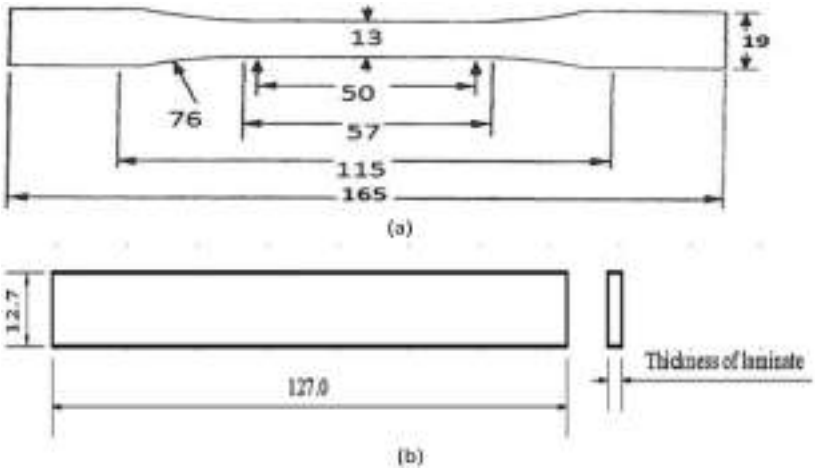

Fig. 1. (a) ASTM D638 Type I Standard tensile specimen. (b) ASTM D790 Method B standard bending specimen.

Fig. 2. Tensile and bending specimens fabricated using FDM.

samples were visually inspected to ensure dimensional accuracy and the absence of printing defects prior to testing. This investigation is a screening study at coupon level. Standardized samples were tested in tension and bending to measure properties at the material level. No full-socket structural testing or ISO 10328 pass/fail evaluation was performed; Therefore, the results are intended for comparative material selection rather than clinical safety validation.

Table 1. FDM printing parameters for PLA and PETG specimens.

Parameter	Printing features
Printer	Anycubic Kobra 2 Max
Nozzle material/diameter	Brass/0.60 mm
Layer height	0.18 mm
Line width (default)	0.60 mm
First-layer line width	0.59 mm
Outer wall line width	0.60 mm
Inner wall line width	0.60 mm
Infill density	100%
Infill/raster pattern	Rectilinear
Top/bottom solid layers	5/3
Print orientation	0°
Nozzle temperature (1st/other)	260/260°C
Bed temperature (Textured PEI, 1st/other)	80/80°C
First-layer speed	60 mm/s
First-layer infill speed	60 mm/s
Outer wall speed	60 mm/s
Inner wall speed	60 mm/s
Sparse infill speed	50 mm/s
Initial layer travel speed	100%
Minimum print speed	20 mm/s
Part cooling fan speed	0% (min/max thresholds)
Support	None
Post-processing	None
Conditioning before testing	24 h at room temperature

2.1. Experimental work

Test specimens for PLA and PETG were fabricated using a fused filament fabrication (FFF) 3D printing process (Fig. 2). All samples were printed using a 100% infill density to eliminate the influence of internal porosity on mechanical performance. A 0.6 mm nozzle diameter was used, and all printing parameters were kept constant for both materials to ensure a fair comparison (Table 1).

A rectangular wooden mold was made for the laminated composite material (Fig. 3a), which was subsequently filled with plaster to form a mold for lamination (Fig. 3b)

The lamination process was carried out using a composite layup consisting of twelve layers of Perlon, with Polyvinyl alcohol (PVA) used as a release and isolation. The layers were bonded using epoxy resin in combination with a compatible hardener (Fig. 4), ensuring proper impregnation and structural integrity of the laminated composite (Table 2).

Following lamination and curing, the composite plate was removed from the mold carefully. The resulting edges were then smoothed and the plate was

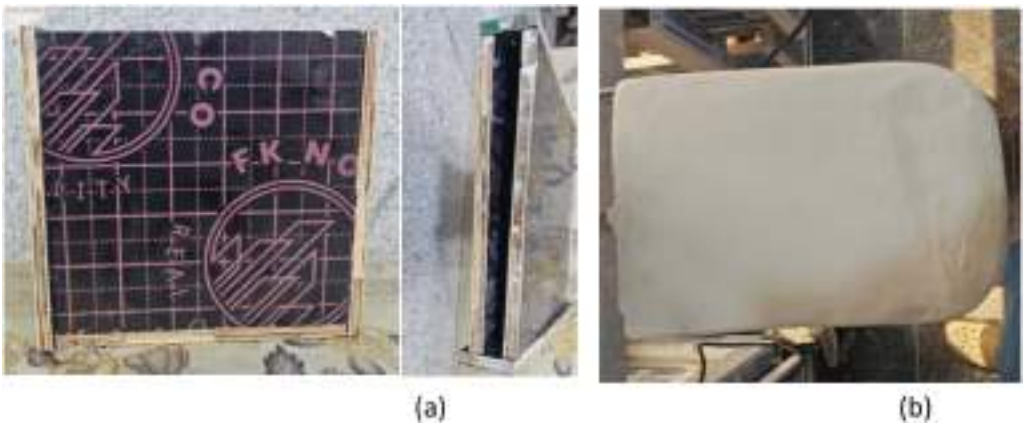

Fig. 3. (a) Wooden mold. (b) Plaster mold.

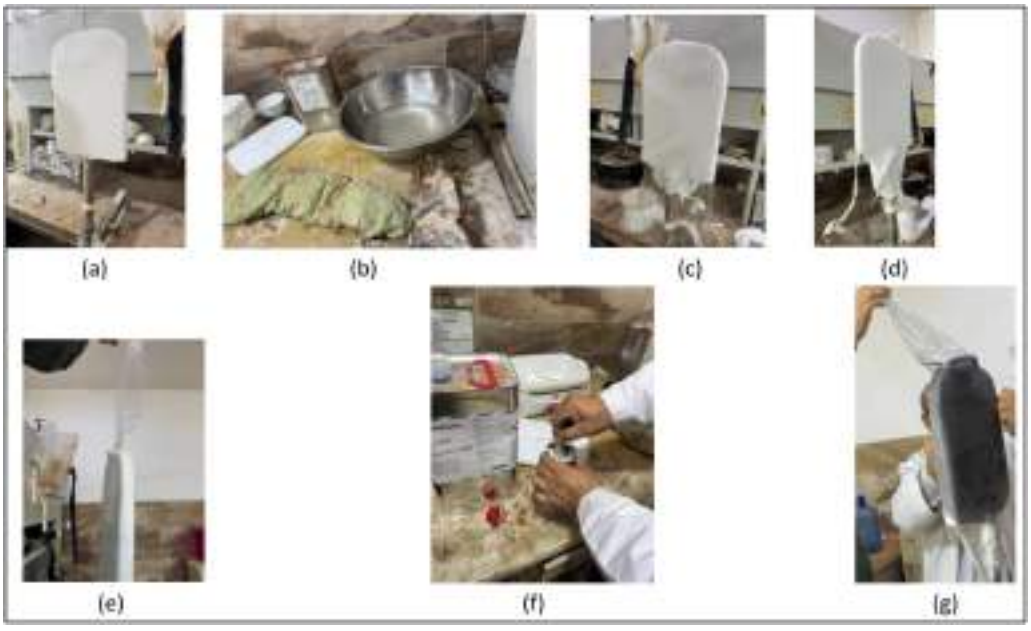

Fig. 4. (a) Preparation of mold. (b) PVA wet. (c) Putting first PVA on the mold. (d) Add perlon layers on the mold. (e) Putting second PVA. (f) Mixing the resin with hardener and color. (g) Pouring the mixture on the layers.

Table 2. Final layup schedule for perlon-epoxy laminated coupons.

Item	Specification
Mold	Rectangular wooden mold, waxed and sealed
Release/isolation	PVA film used as release layer to prevent bonding to the mold and confine resin within the laminate
Reinforcement	Perlon fabric, 12 layers
Layup sequence	PVA/Perlon × 12/PVA
Resin system	Epoxy resin + compatible hardener
Mixing ratio	Resin: hardener = 100:3 (by weight)
Impregnation method	Hand lay-up (wet lay-up), manual consolidation (vacuum bagging, perlon-strip squeegee)
Cutting to specimens	Coupons cut and trimmed to ASTM D638 and ASTM D790 specimen dimensions

cut into standard test specimens for tensile (ASTM D638 Type I) and bending (ASTM D790 Method B) tests, following the same standards used for the 3D-printed materials (Fig. 5).

This approach ensured consistency in specimen geometry and testing conditions across all three material systems, enabling a reliable mechanical comparison and objective material selection.

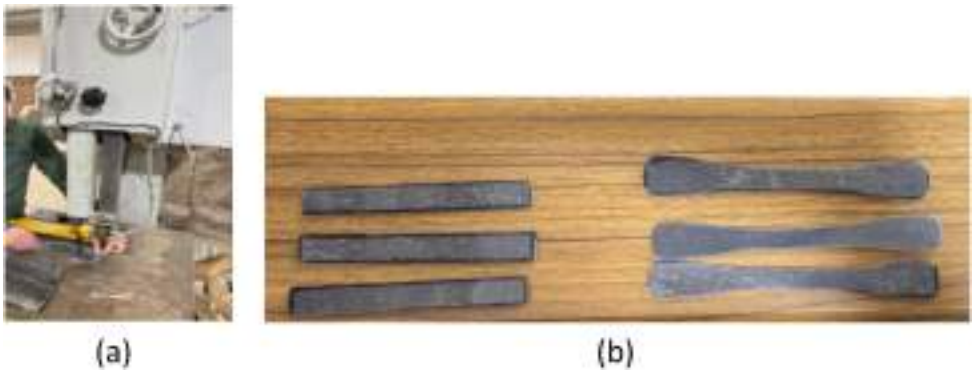

Fig. 5. (a) Cutting process of composite plate. (b) Tensile and bending lamination specimens.

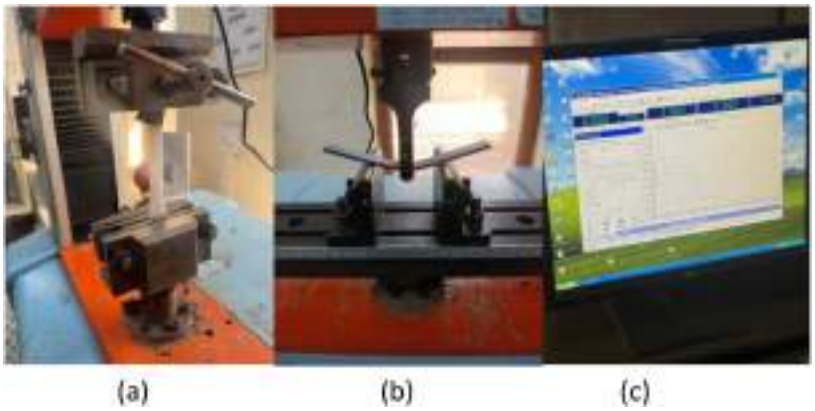

Fig. 6. (a) Tensile test machine. (b) Bending test machine. (c) Visual data screening.

Following specimen fabrication, mechanical evaluation was conducted using two standard laboratory tests: a tensile test (Fig. 6a) and a three-point bending test (Fig. 6b). Each material group (PLA, PETG, and laminated composite) was tested using three specimens per test type. During testing, the load–deformation response was recorded and later used to generate the corresponding stress–strain and load–displacement curves for analysis (Fig. 6c). In addition to the numerical data, photographic documentation was taken throughout the experiments to capture the physical behavior of the specimens.

For tensile testing, images were recorded after fracture to document the failure location and fracture appearance for each sample (Fig. 7a). For bending tests, photographs were taken to illustrate the deformation profile and any visible damage or cracking during and after loading (Fig. 7b). These visual observations are presented alongside the test specimens to support interpretation of the experimental outcomes prior to reporting the quantitative results.

A simplified finite element analysis (FEA) was performed in ANSYS Workbench (Static Structural) to provide additional verification elements for the coupon level tests. ASTM-like tensile (dog-bone) and three-point bending bar geometries were modeled as linear elastic, isotropic solids using experimentally measured material properties. The boundary conditions replicated the laboratory setup: one end of the tensile specimen was clamped while a distal axial load was applied to the opposite grip; For bending, the specimen was supported with a central downward load. Tetrahedral meshing was used with local

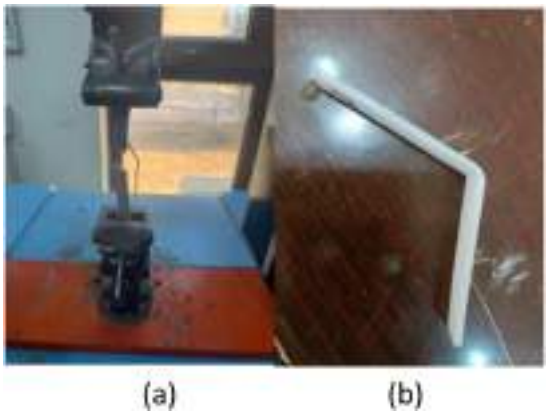

Fig. 7. (a) Fracture mode of tensile specimens. (b) Deformation mode of bending specimens.

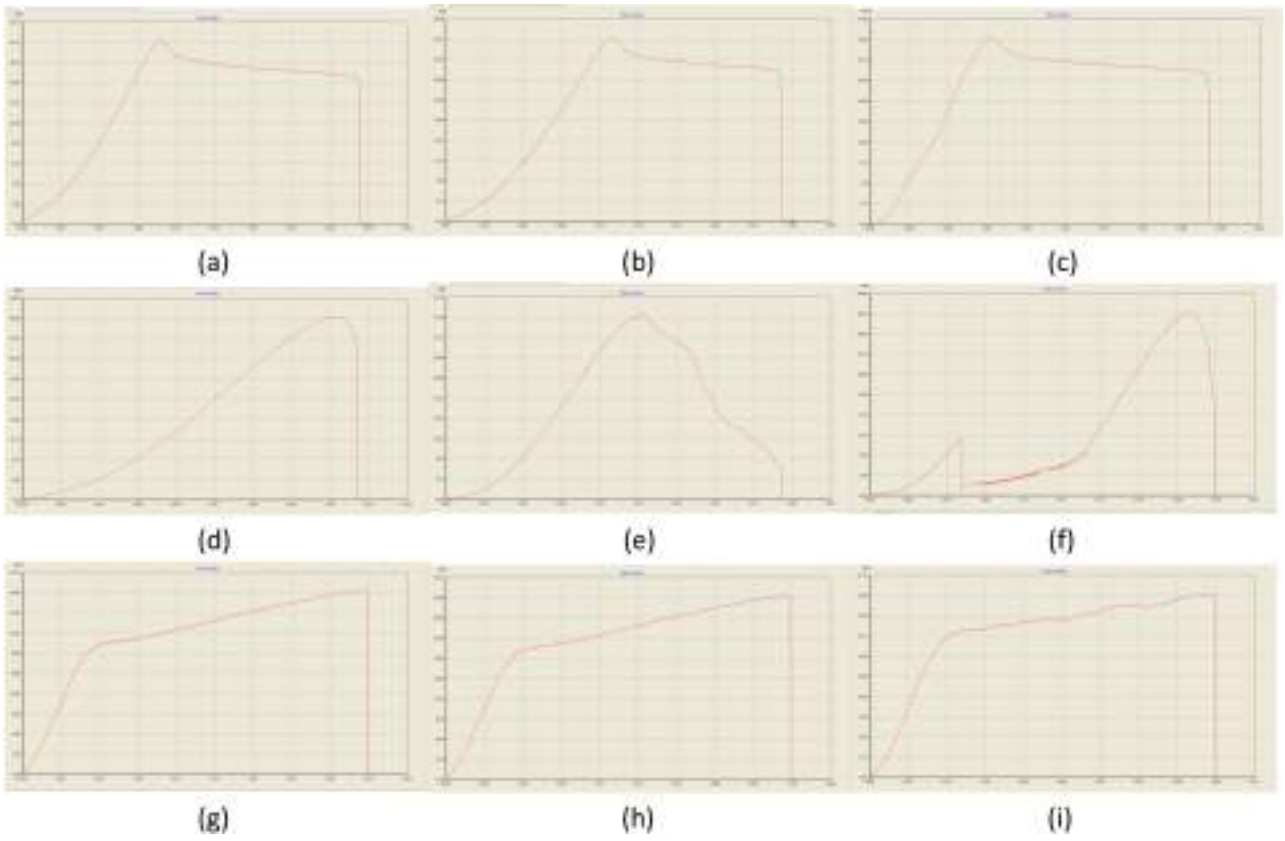

Fig. 8. Tensile stress–strain curves of the specimens: (a) PLA sample 1, (b) PLA sample 2, (c) PLA sample 3, (d) PETG sample 1, (e) PETG sample 2, (f) PETG sample 3, (g) Lamination sample 1, (h) Lamination sample 2, and (i) Lamination sample 3.

refinement in gauge/loaded areas. The primary outputs were von-Mises stress contours and maximum deflection.

Statistical analysis was performed to support comparisons between materials. Results are reported as mean ± standard deviation (SD) for each trait ($n = 3$). Given the small sample size, normality was not assumed; Therefore, group differences were evaluated using the Kruskal–Wallis's test, followed by Dunn's post-hoc pairwise comparisons with Bonferroni correction when appropriate. A significance level of $p < 0.05$ was used. The statistical results are interpreted as exploratory evidence to complement the mechanical trends observed in the stress-strain curves.

3. Results and discussion

Standardized coupon specimens were tested in tension (ASTM D638) and three-point bending (ASTM D790) to compare FDM-printed PLA and PETG with the laminated composite (Perlon–resin). Representative stress–strain curves for each material are provided in the Tensile curves (Fig. 8) and Flexural curves (Fig. 9), while the extracted mechanical properties are summarized in Table 3 (tensile) and Table 4 (flexural). In tensile loading, the materials showed clearly different stiffness and yielding behavior, reflecting the intrinsic polymer response and (for the laminate) the fabric–matrix load sharing, similar trends were observed in bending, where socket-relevant resistance to flexure is critical. This approach is consistent with how many studies report baseline material performance before moving to full-socket structural validation (e.g., ISO 10328-type testing).

In flexural loading, PETG exhibited the highest bending strength among the tested groups, while PLA showed the highest flexural stiffness (modulus), and the Perlon–resin laminate (without carbon reinforcement in this batch) presented the lowest flexural resistance and earlier yielding. These results are meaningful for socket selection because socket walls and distal regions experience combined bending and compression during stance, and materials with higher flexural strength/yield typically tolerate service loads with a larger safety margin. For FDM materials, tensile strength and stiffness are highly sensitive to printing parameters (e.g., temperature, raster strategy, layer height, and inter-layer bonding), and

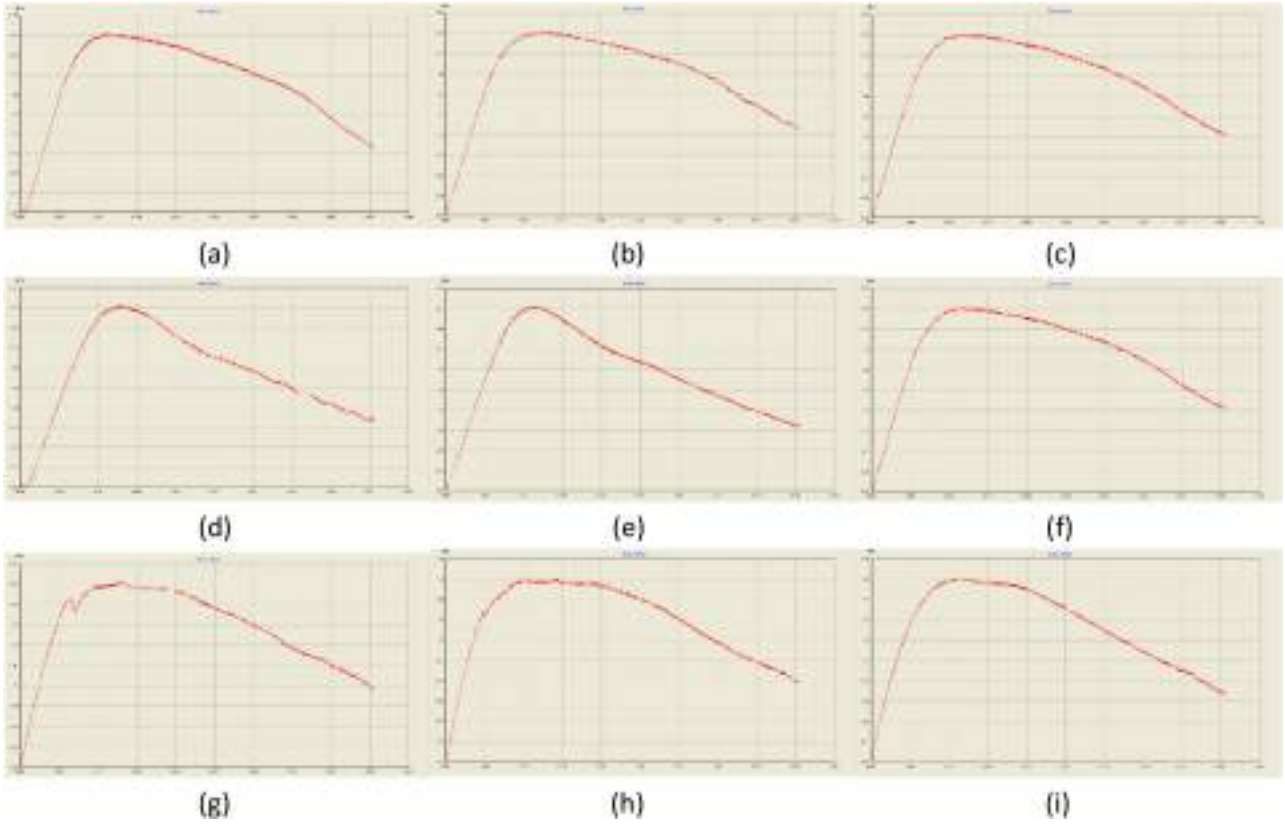

Fig. 9. Bending stress–strain curves of the specimens: (a) PLA sample 1, (b) PLA sample 2, (c) PLA sample 3, (d) PETG sample 1, (e) PETG sample 2, (f) PETG sample 3, (g) Lamination sample 1, (h) Lamination sample 2, and (i) Lamination sample 3.

Table 3. Tensile properties (ASTM D638), mean ± SD (n = 3).

Material	Sample	Young's modulus, E (GPa)	Yield strength, σy (MPa)	Ultimate tensile strength, UTS (MPa)
PLA	1	0.322	28.28	35.24
	2	0.285	28.78	34.62
	3	0.481	15.07	34.27
	Mean ± SD (n=3)	**0.363 ± 0.104**	**24.04 ± 7.78**	**34.71 ± 0.49**
PETG	1	0.315	21.66	36.95
	2	0.325	21.22	38.34
	3	0.307	12.78	40.84
	Mean ± SD (n=3)	**0.316 ± 0.009**	**18.55 ± 5.00**	**38.71 ± 1.97**
Lamination (Perlon-resin)	1	0.164	18.71	30.28
	2	0.172	16.5	28.9
	3	0.185	3.00	25.80
	Mean ± SD (n = 3)	**0.1737 ± 0.0106**	**12.74 ± 8.5**	**28.33 ± 2.29**
Kruskal–Wallis H(2)		**5.42**	**2.22**	**7.20**
p-value		**0.0665**	**0.3292**	**0.0273**

variations in these settings can reduce the effective load-bearing area through voids and imperfect fusion, resulting in lower UTS and earlier yielding compared with idealized or datasheet values [23].

The near-threshold p-values observed for Ef and σfy suggest a potential physical effect that may become statistically evident with larger sample sizes.

The FE model reproduced the expected stress concentration patterns for both tests. In tension, the maximum stress occurred at the gage/shoulder transition, which is consistent with typical failure locations in the ASTM tensile coupons. In bending, the maximum stress developed at the mid-stress tensile surface under the central load, which corresponds to the three-point bending stress distribution (Fig. 10). Under the same bending boundary conditions, the predicted ranking of peak stress and deflection was consistent with experimental trends (PETG > PLA >

Table 4. Flexural properties (ASTM D790), measured values and mean ± SD (n = 3).

Material	Sample	Flexural modulus E_f (GPa)	Flexural yield σf_y (MPa)	Flexural strength σf_{max} (MPa)
PLA	1	2.19	50.92	60.13
	2	1.96	50.59	56.45
	3	2.05	47.65	55.53
	Mean ± SD	**2.07 ± 0.12**	**49.72 ± 1.80**	**57.37 ± 2.44**
PETG	1	1.70	59.63	70.82
	2	1.73	61.42	73.66
	3	1.73	50.21	67.37
	Mean ± SD	**1.72 ± 0.02**	**57.09 ± 6.02**	**70.62 ± 3.15**
Lamination (Perlon–resin)	1	1.54	18.73	43.80
	2	1.87	26.68	44.73
	3	1.87	30.32	44.26
	Mean ± SD	**1.76 ± 0.19**	**25.24 ± 5.93**	**44.26 ± 0.47**
Kruskal–Wallis H(2)		**5.695**	**5.956**	**7.2**
p-value		**0.0580**	**0.0509**	**0.0273**

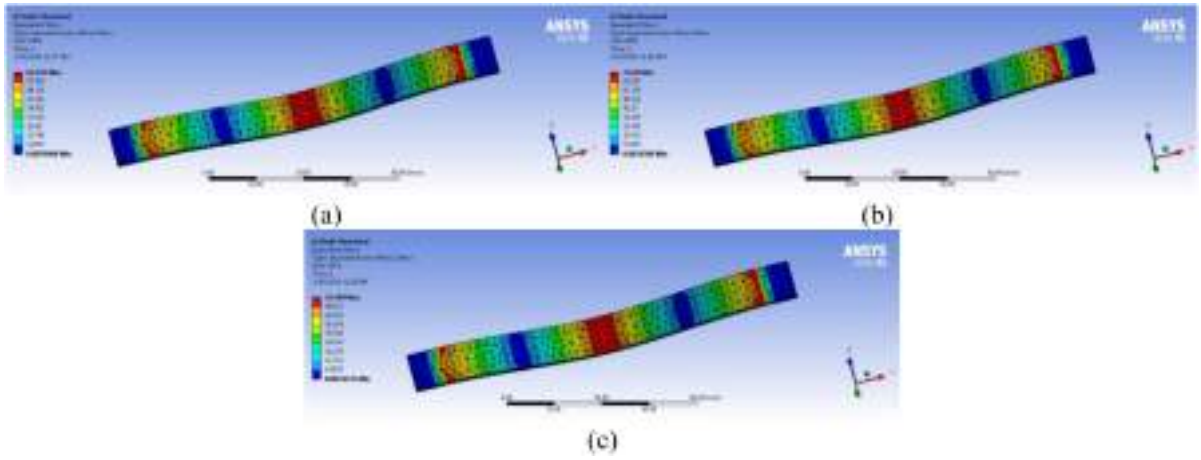

Fig. 10. Peak stress in three-point bending occurs at the midspan tensile surface: (a) PLA, (b) PETG, (c) Lamination.

lamination for peak stress, while PLA showed lower deflection indicating higher stiffness). Overall, FEA was used as a qualitative/technical verification of stress distribution and relative compliance rather than direct prediction of ultimate failure load.

The tensile and flexural results (Tables 3 and 4) and the corresponding stress–strain curves (Figs. 8 and 9) highlight clear differences in stiffness, yielding behavior, and strength among the tested material routes. This is expected because FDM-printed thermoplastics behave as layered, process-dependent polymers, whereas laminated composites behave as fabric–matrix systems whose performance depends strongly on reinforcement architecture and fiber content. At the socket level, these differences translate into changes in how the structure resists the combined loading that occurs during gait, where heel strike is widely reported as one of the most critical phases due to abrupt load transfer and local stress concentration near distal/posterior regions [24]. In tension, the extracted properties summarize how each material balances rigidity (Young's modulus) with load-carrying capacity (yield and UTS). The PLA and PETG coupons represent typical FDM thermoplastic behavior, an initial linear elastic region followed by nonlinearity (associated with yielding and/or damage accumulation), then peak stress and fracture. In the literature, FDM tensile behavior is strongly influenced by build orientation and inter-layer bonding, sockets or coupons printed at certain orientations can meet ISO 10328 static requirements, while other orientations fail prematurely, indicating that polymer performance is not purely material but also manufacturing [25]. Flexural testing provides a practical proxy for socket wall behavior because sockets experience bending-dominated deformation during stance and transitions, especially around trimlines and distal regions. In our dataset, PETG demonstrated the highest flexural strength, which supports its reputation as a tougher thermoplastic suitable for functional printed parts when bending resistance is prioritized. Meanwhile, PLA showed a higher flexural modulus, indicating a stiffer response (less deflection under the same bending load). This stiffness can

help maintain dimensional stability, but in socket applications it may also increase the risk of abrupt cracking if stress concentrators exist or if the loading becomes impact-like. These strength vs. stiffness trade-offs are consistent with broader AM findings, where the flexural behavior of PETG is frequently improved or degraded depending on process parameters, and systematic optimization studies report strong dependence of PETG flexural strength on infill, temperature, and raster strategy using ASTM D790-based testing [26, 27]. The relatively low flexural yield/strength of the laminated specimens in the current batch should be interpreted carefully because the laminate was produced without carbon fiber reinforcement. In prosthetic practice and in socket research, carbon-fiber lamination is commonly used to raise stiffness and ultimate strength. Therefore, a Perlon–resin laminate represents a baseline composite rather than the performance ceiling of traditional lamination. When carbon reinforcement is included, laminated sockets generally exhibit superior ultimate strength under ISO-based structural loading compared with polymer-only solutions [28]. From an engineering perspective, socket materials are often judged by their ability to provide sufficient strength at a minimum wall thickness, supporting a favorable strength-to-weight ratio while maintaining stiffness for stable load transfer. Current coupon results can therefore inform preliminary safety margins for a given design thickness, although definitive margins should be confirmed by socket-level structural testing under ISO-based loading [25, 28]. High-risk failure regions typically include the distal end/attachment region and trim line transitions with high curvature, where local stress concentrations can accelerate crack initiation during repeated bending [28]. Taken together, the results suggest a practical hierarchy in behavior: PETG offers stronger bending resistance (desirable against flexural failure), PLA offers higher stiffness (desirable for shape stability but potentially less forgiving under concentrated stresses), and the tested Perlon–resin laminate provides a baseline composite response that would be expected to increase substantially if carbon reinforcement were reintroduced.

Finally, it is important to emphasize that ASTM D638 and ASTM D790 standardize the test method at the coupon level, whereas clinical safety for sockets is typically evaluated at the component level using standards such as ISO 10328. Accordingly, the present results support material selection and benchmarking, while socket-level verification under standardized structural loading is recommended before definitive clinical use. A limitation of this screening study is the modest sample size (n = 3 per group), which may reduce statistical power; Therefore, the results are primarily interpreted to identify trends at the content level and guide subsequent validation at the socket level.

4. Conclusion

This study compared FDM-printed PLA and PETG with a conventional Perlon–resin laminate using standardized tensile (ASTM D638) and flexural (ASTM D790) tests. The coupon-level tensile and flexural results showed that PETG achieved the best flexural strength, while PLA exhibited higher stiffness. These findings support preliminary material selection for prosthetic socket manufacturing. From a practical manufacturing perspective, 3D printing offers clear advantages over lamination in terms of production time, cost, and repeatability, with reduced reliance on highly skilled manual workmanship. In contrast, lamination is labor-intensive, consumes more materials, and is highly sensitive to workmanship; minor processing errors can compromise quality and lead to complete socket rejection. Therefore, FDM printing represents an efficient and scalable route for socket production, while future work should confirm performance at the socket level under standardized structural loading (e.g., ISO-based testing) and investigate reinforcement strategies for critical high-stress regions.

Acknowledgment

Not applicable.

Conflict of interest

The authors declare that there are no conflicts of interest regarding the publication of this paper.

Funding

This research received no external funding.

References

1. M. Wang, Q. Nong, Y. Liu, and H. Yu, “Design of lower limb prosthetic sockets: a review,” *Expert Review of Medical Devices*, 2022-01-02.
2. S. M. M, and A. H. D, “Investigation of Friction for Nanocoated and Uncoated Ti-6Al-4V Substrates via the Modified Pin-on-Disk Technique for Transfemoral Implants - PubMed,” *Journal of biomedical physics & engineering*, vol. 15, no. 2, 04/01/2025.

3. S. Turner and A. H. McGregor, “Perceived Effect of Socket Fit on Major Lower Limb Prosthetic Rehabilitation: A Clinician and Amputee Perspective,” *Archives of Rehabilitation Research and Clinical Translation*, vol. 2, no. 3, 2020/09/01.
4. M. J. Jweeg, Z. S. Hammoudi, B. A. Alwan, M. J. Jweeg, Z. S. Hammoudi, and B. A. Alwan, “Optimised Analysis, Design, and Fabrication of Trans-Tibial Prosthetic Sockets,” *IOP Conference Series: Materials Science and Engineering*, vol. 433, no. 1, 2018-11-01.
5. J. S. S. Manrique, C.C.-D.l Portilla, J. S. Salgado Manrique, and C. Cifuentes-De la Portilla, “Exploring Opportunities for Advancements in Lower Limb Socket Fabrication and Testing: A Review,” *Biomechanics*, vol. 5, no. 3, pp. 64, 2025-09-01.
6. S. M. Hasany, S. Verma, and K. Dhingra, “3D printing prostheses using additive manufacturing and regenerative engineering,” *Journal of Knowledge Learning and Science Technology ISSN: 2959-6386 (online)*, vol. 4, no. 1, 2025.
7. Y. Wang, Q. Tan, F. Pu, D. Boone, and M. Zhang, “A Review of the Application of Additive Manufacturing in Prosthetic and Orthotic Clinics from a Biomechanical Perspective,” *Engineering*, vol. 6, no. 11, 2020/11/01.
8. S. Day, “14 - Using rapid prototyping in prosthetics: Design considerations,” In: R. Narayan, Ed., *Rapid Prototyping of Biomaterials (Second Edition)*. Woodhead Publishing, 2020, pp. 325–38.
9. Y. J. Choo, J. H. Kim, and M. C. Chang, “Three-dimensional printing technology applied to the production of prosthesis: A systemic narrative review,” *Prosthetics and Orthotics International*, vol. 49, no. 3, June 2025.
10. Z. K. Mashi, “From Metals to Composite Materials: A Comprehensive Review of Materials Used in Prosthetic Limb Manufacturing,” *Journal of University of Babylon for Engineering Sciences*, vol. 33, no. 4, 2025/08/28.
11. A. Jain, “3D Printed Prosthetics: Advancements in Customization and Material Science,” *International Journal of Research in Modern Engineering & Emerging Technology*, 2022.
12. M. vdS, L. V, C. H. S, L. B, and T. J. M, “Strength testing of low-cost 3D-printed transtibial prosthetic socket - PubMed,” *Proceedings of the Institution of Mechanical Engineers Part H, Journal of engineering in medicine*, vol. 236, no. 3, Mar 2022.
13. T. Marinopoulos, S. Li, and V. V. Silberschmidt, “Mechanical performance of 3D printed prosthetic sockets: An experimental and numerical study,” *Procedia Structural Integrity*, vol. 42, 2022/01/01.
14. V. Plesec, J. Humar, P. Dobnik-Dubrovski, and G. Harih, “Numerical Analysis of a Transtibial Prosthesis Socket Using 3D-Printed Bio-Based PLA,” *Materials*, vol. 16, p. 1985, 2023.
15. S. Valvez, A. P. Silva, P. N. B. Reis, S. Valvez, A. P. Silva, and P. N. B. Reis, “Optimization of Printing Parameters to Maximize the Mechanical Properties of 3D-Printed PETG-Based Parts,” Polymers, vol. 14, no. 13, p. 2564, 2022-06-24.
16. B. Štefanovič, B. Lucia, M. Michalíková, R. Hudak, and J. Zivcak, “THE PRODUCTION OF HYBRID PROSTHETIC SOCKETS THROUGH THE INTEGRATION OF 3D PRINTING AND CONVENTIONAL LAMINATION,” *Lékař a technika - Clinician and Technology*, vol. 54, pp. 48–51, 2024.
17. R. Romero, K. A. Costa, C. B. S. Vimieiro, R. Romero, K. A. Costa, C. B. S. Vimieiro, *et al.*, “Open-source hand prosthesis: evaluation of mechanical feasibility and additive manufacturing potential,” *Journal of Complexity in Health Sciences*, vol. 7, no. 2, 2024-09-25.
18. M. K. Owen and J. D. DesJardins, “Transtibial Prosthetic Socket Strength: The Use of ISO 10328 in the Comparison of Standard and 3D-Printed Sockets,” *JPO: Journal of Prosthetics and Orthotics*, vol. 32, no. 2, April 2020.
19. R. F. Martins, R. Branco, M. Martins, W. Macek, Z. Marciniak, R. Silva, *et al.*, “Mechanical Properties of Additively Manufactured Polymeric Materials—PLA and PETG—For Biomechanical Applications,” *Polymers*, vol. 16, p. 1868, no. 13, 2024-06-29.
20. M.-H. Hsueh, C.-J. Lai, S.-H. Wang, Y.-S. Zeng, C.-H. Hsieh, C.-Y. Pan, *et al.*, “Effect of Printing Parameters on the Thermal and Mechanical Properties of 3D-Printed PLA and PETG, Using Fused Deposition Modeling,” *Polymers*, vol. 13, no. 11, p. 1758, 2021-05-27.
21. T. Appalsamy, S. L. Hamilton, M. J. Kgaphola, T. Appalsamy, S. L. Hamilton, and M. J. Kgaphola, “Tensile Test Analysis of 3D Printed Specimens with Varying Print Orientation and Infill Density,” *Journal of Composites Science*, vol. 8, no. 4, 2024-03-26.
22. S. Kumar, I. Singh, S. S. R. Koloor, D. Kumar, M. Y. Yahya, S. Kumar, *et al.*, “On Laminated Object Manufactured FDM-Printed ABS/TPU Multimaterial Specimens: An Insight into Mechanical and Morphological Characteristics,” *Polymers*, vol. 14, no. 19, 2022-09-28.
23. M. Doshi, A. Mahale, S. Kumar Singh, and S. Deshmukh, “Printing parameters and materials affecting mechanical properties of FDM-3D printed Parts: Perspective and prospects,” *Materials Today: Proceedings*, vol. 50, pp. 2269–75, 2022.
24. D. F. Fitriyana, S. Palanisamy, Y. S. Wicaksana, S. Anis, J. P. Siregar, T. Cionita, *et al.*, “Mechanical performance analysis of a 3D printing-based transtibial prosthetic socket against the gait cycle using the finite element method,” *RSC Advances*, vol. 15, no. 30, pp. 24150–66, 2025.
25. A. F. Che Manan, M. J. Abd Latif, M. Narasamman, M. Musa, M. N. Abdul Rahman, G. D. Lim, *et al.*, “Effect of printing orientation on structural strength of 3D-printed polylactic acid prosthetic socket using fused deposition modeling,” *Prosthet Orthot Int*, 2025.
26. N. A. Fountas, I. Papantoniou, J. D. Kechagias, D. E. Manolakos, and N. M. Vaxevanidis, “Modeling and optimization of flexural properties of FDM-processed PET-G specimens using RSM and GWO algorithm,” *Engineering Failure Analysis*, vol. 138, p. 106340, 2022.
27. N. A. Fountas, I. Papantoniou, J. D. Kechagias, D. E. Manolakos, N. M. Vaxevanidis, Eds., “Experimental investigation on flexural properties of FDM-processed PET-G specimen using response surface methodology,” *MATEC Web of Conferences*, EDP Sciences, 2021.
28. J. K. Oleiwi, Q. A. Hamad, and S. A. Abdulrahman, “Flexural, impact and max. shear stress properties of fibers composite for prosthetic socket,” *Materials Today: Proceedings*, vol. 56, pp. 3121–8, 2022.